

Scaling properties of azimuthal anisotropy of mesons and baryons at RHIC

Arkadij Taranenko¹ for the PHENIX Collaboration

¹ Department of Chemistry, SUNY Stony Brook,
11790 Stony Brook, USA

Abstract. Detailed measurements of the azimuthal anisotropy (\tilde{v}_2) for identified charged particles are reported as a function of transverse momentum (p_T) and centrality for Au+Au collisions at $\sqrt{s_{NN}}=200$ GeV. The measurements indicate clear evidence for eccentricity and particle flavor scaling over a broad range of centralities and transverse rapidity y_T , indicating a hydrodynamical origin of the fine structure of azimuthal anisotropy at RHIC. The observed scaling supports the picture of a suddenly hadronizing (recombining) fluid of quarks. An apparent breaking of flavor scaling at relatively large values of y_T points to an important change in the mechanism for particle emission.

Keywords: RHIC, PHENIX, azimuthal anisotropy, elliptic flow, Au+Au
PACS: specifications see, e.g. <http://www.aip.org/pacs/>

1. Introduction

During the early stages of an ultra-relativistic heavy-ion collision, an extremely high energy density system, possibly consisting of a new phase of nuclear matter, is expected to be formed [1, 2, 3, 4, 5]. The dynamical evolution of this matter is predicted to reflect its properties [1, 2, 3]. Consequently, much effort is currently centered on the study of reaction dynamics at the Relativistic Heavy Ion Collider (RHIC). Azimuthal correlation measurements constitute an important probe for reaction dynamics. They serve as a “barometric sensor” for pressure gradients developed in the collision and hence yield insight into crucial issues of thermalization and the equation of state (EOS) [6, 7, 8]. They provide important constraints for the density of the medium and the effective energy loss of partons which traverse it [9, 10]. They can even provide valuable information on the gluon saturation scale in the nucleus [11].

Azimuthal correlation measurements show significant harmonic strength at mid-rapidity with characteristic dependencies on p_T and centrality [12, 13, 14, 15]. The

anisotropy of this harmonic pattern is typically characterized by the second order Fourier coefficient,

$$v_2 = \left\langle e^{i2(\phi_1 - \Phi_{RP})} \right\rangle, \quad (1)$$

where ϕ_1 represents the azimuthal emission angle of an emitted particle and Φ_{RP} is the azimuth of the reaction plane. The brackets denote statistical averaging over particles and events. A large amount of available data for Au+Au collisions at $\sqrt{s_{NN}} = 62.4, 130, \text{ and } 200 \text{ GeV}$ [12, 13, 15, 16, 17] indicate that the magnitude and trends of $\check{2}$ (for $p_T \lesssim 2.0 \text{ GeV}/c$) are under-predicted by hadronic cascade models supplemented with string dynamics [18], but are well reproduced by models which incorporate hydrodynamic flow [1, 7]. This has been interpreted as evidence for the production of a thermalized state of partonic matter [1, 2, 3]. If this is indeed the case, then the fine structure of azimuthal anisotropy (ie. its detailed dependence on centrality, transverse momentum, particle type, higher harmonics, etc) should reflect the scaling ‘‘laws’’ predicted by ideal hydrodynamics.

In this work we use detailed differential $\check{2}$ measurements to test for such scaling ‘‘laws’’ and the onset of competing mechanisms.

2. Hydrodynamic scaling

An important scaling prediction of hydrodynamic theory is exemplified by the exact analytic hydro solutions [19] exploited in the Buda-Lund model [20]. For harmonic flow, the model gives:

$$v_{2n} = \frac{I_n(w)}{I_0(w)}, n = 1, 2, \dots, w = \frac{p_t^2}{4\bar{m}_t} \left(\frac{1}{T_y} - \frac{1}{T_x} \right), \quad (2)$$

where $I_{0,n}$ are modified Bessel-functions, \bar{m}_t is an average of the rapidity dependent transverse mass (at mid-rapidity, $\bar{m}_T = m_T$), and T_x and T_y are direction (x and y) dependent slope parameters:

$$T_x = T_0 + \bar{m}_t \dot{X}_f^2 \frac{T_0}{T_0 + \bar{m}_t a}, \quad (3)$$

$$T_y = T_0 + \bar{m}_t \dot{Y}_f^2 \frac{T_0}{T_0 + \bar{m}_t a}. \quad (4)$$

Here, \dot{X}_f and \dot{Y}_f gives the transverse expansion rate of the fireball at freeze-out, and $a = (T_0 - T_s)/T_s$ is its transverse temperature inhomogeneity, characterized by the temperature at its center T_0 , and at its surface T_s . The important prediction of Eq. 2 is that the relatively complicated fine structure of azimuthal anisotropy can be scaled to a single function. An illustration of this fact can be made for particle flavor scaling via substitution of the transverse rapidity [21], $y_T = \sinh^{-1}(p_T/m)$ in Eq. 2 to give

$$v_2 = k_1 y_T^2 \frac{m}{T_0} \left(1 + \frac{k_2 T_0}{k_1 m} + \frac{k_3 T_0^2}{k_1 m} \dots \right), \quad (5)$$

where, $k_1, k_2, k_3\dots$ are largely governed by the expansion rate. Close inspection of the leading term in Eq. 5 indicates that v_2 for different particle species should scale with $y_T^{fs} = k_m \cdot y_T^2 m$. Here k_m is a mass dependent factor which is $\simeq 1$ for relatively heavy particles. It is straightforward to show that hydrodynamics also predicts that v_2 should scale with the spatial eccentricity $\varepsilon = (Y^2 - X^2)/(Y^2 + X^2)$, of the overlap between the two colliding gold nuclei and the higher harmonic $v_4 \sim \frac{1}{2}v_2^2 + k_m y_T^4$.

3. Analysis

The present analysis is based on $\simeq 22$ M minimum bias Au+Au events obtained with the PHENIX detector at $\sqrt{s_{NN}} = 200$ GeV during the second running period (2002) at RHIC. Charged tracks were detected in the east and west central arms of PHENIX [24, 26], each of which subtends 90° in azimuth ϕ , and ± 0.35 units of pseudo-rapidity η . Track reconstruction was accomplished at each collision energy via pattern recognition using a drift chamber (DC) followed by two layers of multi-wire proportional chambers with pad readout (PC1 and PC3) located at radii of 2 m, 2.5 m and 5 m respectively [24, 26]. The collision vertex z along the beam direction was constrained to be within $|z| < 30$ cm. A confirmation hit within a 2σ matching window was required in PC3 and the electromagnetic calorimeter (EMC PbSc) or the time-of-flight detector (TOF), to eliminate most albedo, conversions, and decays. Particle momenta were measured with a resolution of $\delta p/p = 0.7\% \oplus 1.0\% p$ (GeV/c).

Event centralities were obtained via a series of cuts in the space of BBC versus ZDC analog response; they reflect percentile cuts on the total interaction cross section [25]. Estimates for the number of participant nucleons N_{part} , were also made for each of these cuts following the Glauber-based model detailed in Ref. [13].

In this analysis the combination of the TOF detector and six sectors of the (EMC PbSc) was used to identify charged particles. Particle time-of-flight was measured using the TOF (or EMC) and the collision time defined by beam counters (BBC). A timing resolution of $\simeq 120$ ps and $\simeq 370$ -400 ps was obtained for the TOF and the EMC (PbSc) respectively. This allowed meson (π^\pm, K^\pm) and baryon (p, \bar{p}) separation up to a $p_T \simeq 3.5$ GeV/c with the TOF detector and up to 2.5 GeV/c with the (EMC PbSc).

The differential $v_2(p_T, centrality)$ measurements were obtained via the reaction plane technique which correlates the azimuthal angles of charged tracks detected in the central arms with the azimuth of an estimated event plane Φ_2 , determined via hits in the North and South BBC's located at $|\eta| \sim 3 - 3.9$ [15, 27]. Due the large rapidity gap ($\sim 3 - 3.9$ units) between the particles used for reaction plane determination and the mid-rapidity particles correlated with this plane, one expects that the latter correlations are less influenced by non-flow contributions especially for $p_T < 3.0$ GeV/c. The estimated resolution of the combined reaction plane from both BBC's [15, 27] has an average of 0.33 over centrality with a maximum

of about 0.42 for Au+Au collisions at $\sqrt{s_{NN}}=200$ GeV. Thus, the estimated correction factor, which is the inverse of the resolution for the combined reaction plane, ranges from 2.4 to 5.0.

3.1. v_2 results

Figures 1 and 2 summarize the centrality and p_T dependence of v_2 for charged mesons (π^\pm, K^\pm) and baryons ($p + \bar{p}$) detected in the EMC+TOF respectively.

They give an excellent overview of the the evolution of v_2 as centrality and p_T

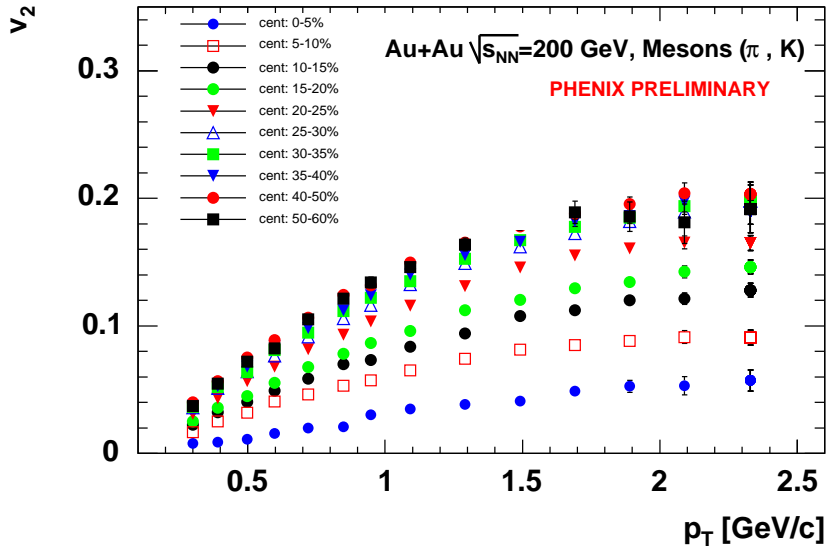


Fig. 1. v_2 vs p_T for charged mesons (π^\pm, K^\pm) for different bins in reaction centrality (top to bottom) 0-5%, 5-10%, ..., 35-40%, 40-50%, 50-60%. The error bars shown indicate statistical errors only. Systematic errors are estimated to be less than 10%.

are varied. The results shown for protons and anti-protons give an especially good view of the evolution away from the well known quadratic dependence of $v_2(p_T)$ (which is also observed in very central collisions for these data) as the collisions become more peripheral. Such a dependence could result from changes in the freeze-out temperatures and/or the radial flow velocity as the collisions become more peripheral.

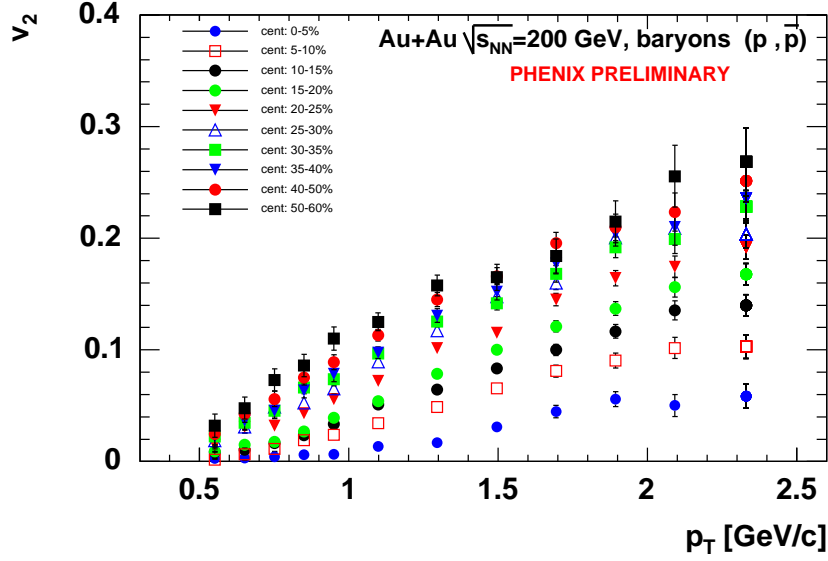


Fig. 2. v_2 vs p_T for charged baryons ($p + \bar{p}$) for different bins in reaction centrality (top to bottom) 0-5%, 5-10%, ..., 35-40%, 40-50%, 50-60%. The error bars shown indicate statistical errors only. Systematic errors are estimated to be less than 10%.

3.2. Eccentricity scaling

As indicated earlier, hydrodynamics [23] predicts eccentricity scaling of the azimuthal anisotropy. To test for this scaling, one can divide the v_2 values obtained at a given centrality by the eccentricity ϵ obtained from a Glauber-based calculation obtained for the same centrality [13]. Alternatively, one can simply divide the differential anisotropy $v_2(N_{part}, p_T)$ obtained at a given centrality by the p_T integrated value for the same centrality selection $v_2(N_{part})$. The underlying idea here is that the integral flow is monotonic and linearly related to the eccentricity over a broad range of centralities [22]. Another advantage of this approach is that the ratio $v_2(N_{part}, p_T)/v_2(N_{part})$ gives a scale invariant variable which automatically reduces the systematic errors associated with an eccentricity evaluation, and the reaction plane resolution.

Fig. 3 shows the v_2 of charged mesons obtained for different centralities scaled by the value of the integral flow obtained for each of these centralities. The figure shows essentially perfect scaling for mesons as would be expected for a process driven largely by the eccentricity of the overlap region of the two colliding nuclei. The results of a similar scaling test for baryons are shown in Fig. 4. Despite a continuous evolution in the shape of v_2 vs p_T with centrality, they indicate a relatively good

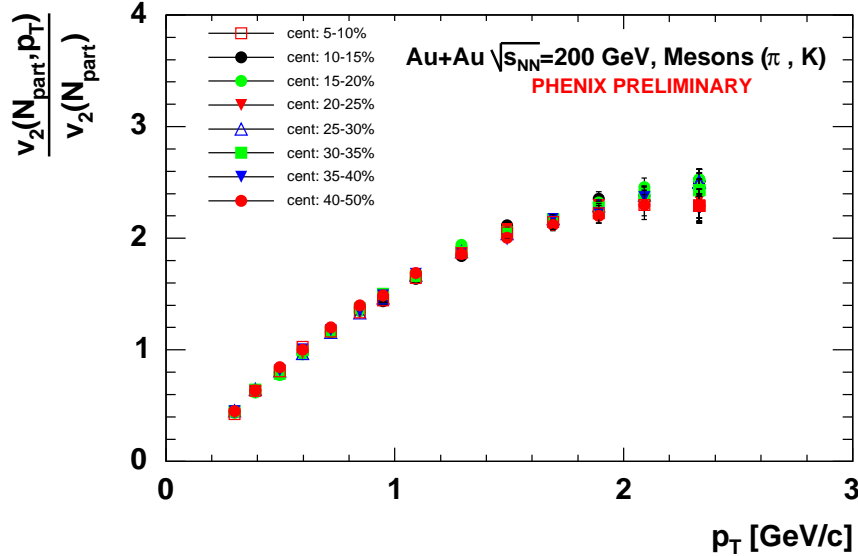


Fig. 3. v_2 vs p_T for charged mesons (for different bins in reaction centrality) scaled by the value of integral flow for each centrality..

scaling for the two centrality ranges: 0-20% (left panel) and 20-50% (right panel).

3.3. Flavor scaling

Following Eq. 5, the scaling variable $y_T^{fs} = k_m \cdot y_T^2 m$, was used to investigate flavor scaling. The results of such a test is summarized in Fig. 5. The left panel of the figure shows a comparison of $v_2(p_T)$ for protons, kaons and pions measured with the TOF detector for the centrality selection 5-30%. The characteristic flavor dependence of v_2 is cleanly evidenced by these data, ie. mass ordering at low momentum and a reversal of the magnitudes of the v_2 values for baryons and mesons for $p_T \sim 1.8-2.0$ GeV/c. The right panel of Fig. 5 and Fig. 6 show that very good scaling of v_2 is achieved with $y_T^{fs} = k_m \cdot y_T^2 m$ in accordance with the predictions of hydrodynamics. Fig. 6 gives an illustration of y_T^{fs} scaling for combined results which include the neutral kaons and lambda hyperons measured by the STAR collaboration. The latter were obtained in Au+Au collisions at $\sqrt{s_{NN}}=200$ GeV for the same centrality selection [16]. Although the data shown in Fig. 6 indicate rather good scaling for all measured particles over a broad range of y_T^{fs} , one can see clear evidence for a break in this scaling for $y_T^{fs} \geq 2$. Such a break could be signaling a change in mechanism for high p_T particles or a break down of ideal hydrodynamic flow.

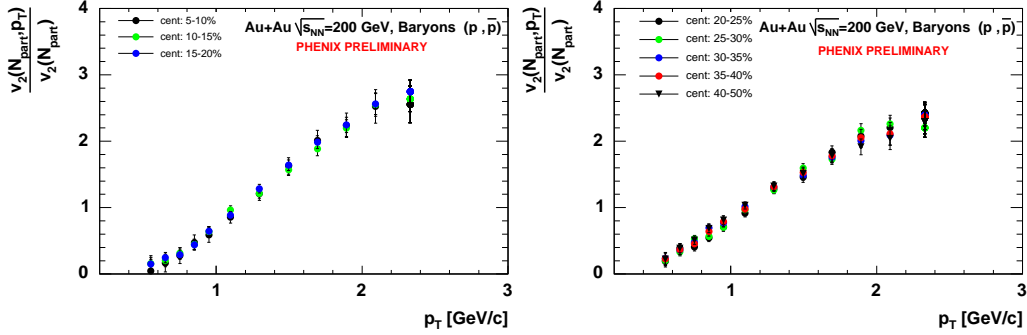


Fig. 4. v_2 vs p_t for charged baryons (for different bins in reaction centrality) scaled by the value of integral flow for each centrality. Left panel corresponds to centrality range 0-20% and right panel to centrality range 20-50%

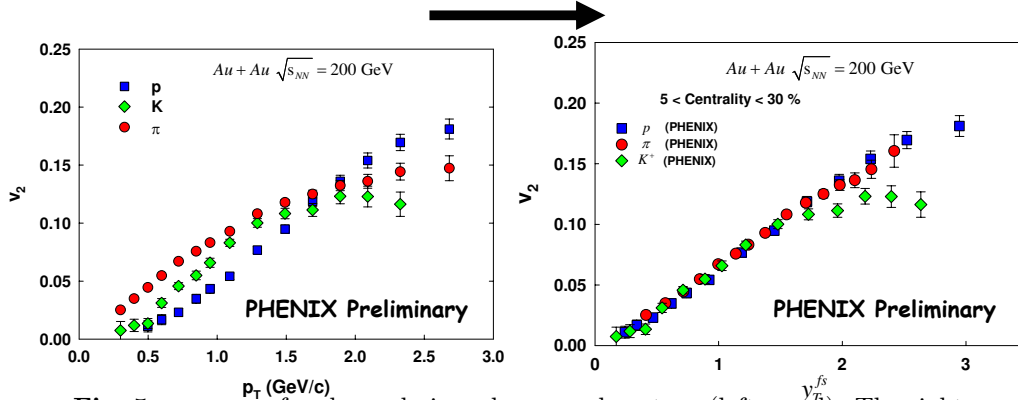


Fig. 5. v_2 vs p_T for charged pions, kaons and protons (left panel). The right panel shows the result of the y_T^{fs} scaling predicted by hydrodynamics. Results are shown for the centrality selection 5-30%.

3.4. Higher harmonic scaling

As was pointed out earlier, ideal hydrodynamics [20] gives and predicts a straightforward scaling relationship between the second harmonic v_2 and the higher harmonics of azimuthal anisotropy (v_4, v_6, \dots). It is easy to show that the leading term of the relationship between v_2 and v_4 can be expressed as

$$v_4 = \frac{1}{2} \cdot v_2^2 + k_5 y_T^4, \quad (6)$$

The measurement of the higher harmonics of azimuthal anisotropy are not available in PHENIX (ongoing). However, we can test the predicted scaling relationship between v_2 and v_4 via data published by the STAR collaboration [28, 29]. Figure

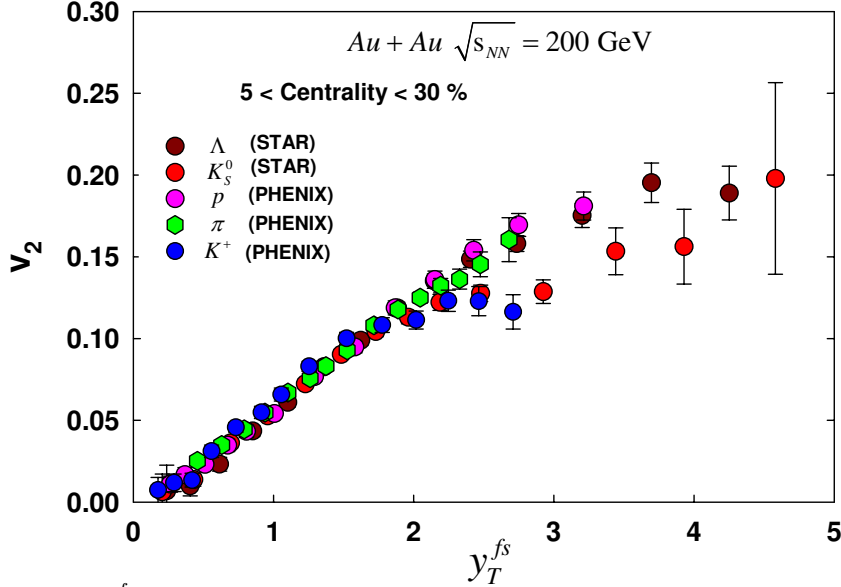


Fig. 6. y_T^{fs} scaling of charged pions, kaons and protons (PHENIX) and neutral kaons and lambdas (STAR) [16]. Results are shown for the centrality selection 5-30%.

7 shows the $(y_T^{fs})^2$ dependence of v_4 for charged particles from Au+Au collisions at $\sqrt{s_{NN}}=200$ GeV and v_2 values scaled according to Eq. 6. The figure indicates rather good agreement between the measured v_4 values and scaled v_2 values over a broad range in y_T^{fs} .

4. Summary and Conclusions

In summary detailed measurements of the fine structure of elliptic flow in Au+Au collisions at $\sqrt{s_{NN}}=200$ GeV measured by PHENIX collaboration at RHIC are presented. They show eccentricity scaling and y_T^{fs} flavor scaling over a broad range of centralities and particle flavors. This observed scaling gives strong support for essentially ideal hydrodynamical flow at RHIC. The observed scaling also supports the picture of a suddenly hadronizing (recombining) fluid of quarks.

Acknowledgment(s)

The author thanks R.A. Lacey, M. Csanád and T. Csörgő for stimulating discussions.

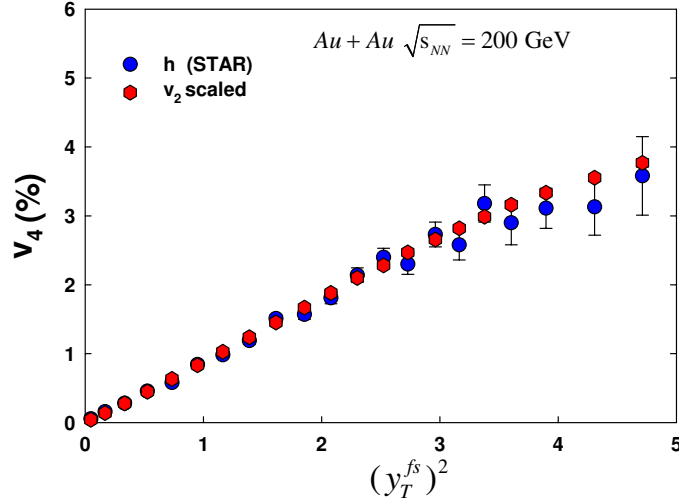


Fig. 7. y_T^{fs} dependence for v_4 of charged particles from Au+Au collisions at $\sqrt{s_{NN}} = 200$ GeV measured by STAR collaboration [28, 29] and these obtained by scaling v_2 values according to Eq. 6

References

1. E.V. Shuryak,(2002) [hep-ph/0405066].
2. M. Gyulassy and L. McLerran, *Nucl. Phys.* **A750** (2005) 30.
3. B. Muller,(2004) [nucl-th/0404015].
4. Proc. of Quark Matter 2004, *J. Phys. G: Nucl. Part. Phys* **30**, (2004)
5. K. Adcox et al., nucl-ex/0410003
6. J. Y. Ollitrault, *Phys. Rev. D* **46**, (1992) 229
7. P. F. Kolb et al, *Nucl. Phys. A* **696**, (2001) 197
8. T. Hirano and Y. Nara, *J. Phys. G* **30**, (2004) S1139
9. M. Gyulassy, I. Vitev and X. N. Wang,*Phys. Rev. Lett.* **86**,(2001) 2537
10. D. Molnar and M. Gyulassy, *Nucl. Phys. A* **697** (2002) 495
11. Y. V. Kovchegov and K. L. Tuchin,*Nucl. Phys. A* **708** (2002) 413
12. C. Adler et al, *Phys. Rev. Lett.* **87**, (2001) 182301
13. K. Adcox et al., *Phys. Rev. Lett.* **89** (2002) 212301
14. N. N. Ajitanand et al, *Nucl. Phys. A* **715** (2003) 765
15. S.S. Adler et al, *Phys. Rev. Lett.* **91** (2003) 182301.
16. J. Adams et al, *Phys. Rev. Lett.* **92**,(2004) 052302
17. S.S. Adler et al, nucl-ex/0411040
18. M. Bleicher and H. Stocker, *Phys. Lett. B* **526** (2002) 309
19. T. Csörgő et al, *Phys. Rev. C* **67**, (2003) 034904
20. M. Csanád, T. Csörgő and B. Lörstad *Nucl. Phys. A* **742** (2004) 80

21. M. Csanád, T. Csörgő, private communication (2004)
22. H. Heiselberg and A. Levi, *Phys. Rev. C* **59** (1999) 2716
23. P. F. Kolb and U. Heinz, 'Quark Gluon Plasma 3'. Editors: R.C. Hwa and X.N. Wang, World Scientific, Singapore., nucl-th/0305084
24. K. Adcox et al., *Nucl. Instrum. Meth. A* **499** (2003) 469
25. K. Adcox *et al.* *Phys. Rev. C* **69** (2004) 024904
26. S. S. Adler et al., *Phys. Rev. C* **69**, (2004) 034909
27. S.S. Adler et al, nucl-ex/0502009
28. *Phys. Rev. Lett.* **92** (2004) 062301
29. J. Adams *et al.* (2004) nucl-ex/0409033.

